Letter to the Editor

Imaging findings of primary vaginal malignancies by dual-layer spectral detector CT: description of two patients

Yuanyuan Cui[1,2#], Zhengwei Zhang[3#], Xiaohui Zhang[4], Baolian Zhao[1], Xiaolei Shi[1], Zhi Zhu[3], Xiaojun Liu[5], Shiyuan Liu[1], Yi Xiao[1]

[1]Department of Radiology, Second Affiliated Hospital of Naval Medical University, Shanghai, China; [2]Department of Radiology, Qingdao Special Servicemen Recuperation Center of PLA Navy, Qingdao, China; [3]Department of Pathology, Second Affiliated Hospital of Naval Medical University, Shanghai, China; [4]Department of Clinical Science, Philips Healthcare Greater, Shanghai, China; [5]Department of Obstetrics and Gynecology, Second Affiliated Hospital of Naval Medical University, Shanghai, China

[#]These authors contributed equally to this work.

Correspondence to: Shiyuan Liu, MD, PhD; Yi Xiao, MD, PhD. Department of Radiology, Second Affiliated Hospital of Naval Medical University, 415 Fengyang Road, Huangpu Distinct, Shanghai 20003, China. Email: cjr.liushiyuan@vip.163.com; xiaoyi@188.com.

Submitted Jun 01, 2023. Accepted for publication Oct 12, 2023. Published online Nov 17, 2023.
doi: 10.21037/qims-23-717
View this article at: https://dx.doi.org/10.21037/qims-23-717

Introduction

Primary vaginal malignancies (PVMs) are rare entities in elderly or postmenopausal women (1-3). The incidence of melanoma is about 0.32–0.79/million and it has a poor prognosis (4), whereas high-grade squamous intraepithelial lesion is a kind of precancerous lesion with a relatively better prognosis. Thus, the early diagnosis is critical. Computed tomography (CT) is commonly used for screening as an alternative to ultrasound and magnetic resonance (MR). However, the unspecific image characteristics and low tissue contrast limit its usage. It has been reported that dual-layer spectral detector CT (DLCT) enabled the detection of occult lesions on conventional CT in many organs such as the pancreas (5), liver (6), and colon (7). In this report, we presented DLCT images of two cases with melanoma and high-grade squamous intraepithelial lesion.

Case presentation

Case 1

A 78-year-old female complained of abnormal vaginal discharge and irregular bleeding for more than 2 months. Cervical biopsy showed squamous cell carcinoma (3 and 9 o'clock of the vaginal wall) in the local hospital. For further diagnosis and treatment, she was admitted in our hospital. Gynecological physical examination showed two masses on the superior 1/3 of the right and left vaginal walls. With virtual monoenergetic images (MonoE) at 40 keV of DLCT (Spectral CT; Philips, Best, Netherlands), an obvious orbicular enhanced lesion appeared on the left wall of the vagina in the arterial phase, and persistent enhancement and clear boundary were revealed in the venous phase (*Figure 1A*). The lesion was also well-defined on the Z-effective map and iodine density (ID) map in the venous phase (*Figure 1B,1C*), with a maximum length of lesion 26 mm on sagittal CT view. However, only a slight enhancement appeared on CT conventional images in the arterial and venous phases (*Figure 1D*), resulting in a misdiagnosis being made upon the first image reading process. The corresponding quantitative parameters of each phase are shown in *Table 1*. The patient underwent a magnetic resonance imaging (MRI) examination 7 days later (*Figure 1E,1F*). A nodule was found on the left vaginal wall with a maximum length on the sagittal MR view of about 21 mm (*Figure 1F*).

Uterine, bilateral adnexectomy, and pelvic lymph node dissection were performed. The pathological diagnosis (*Figure 2A,2B*) was high-grade squamous intraepithelial lesion with focal carcinogenesis. The immunohistochemical results (*Figure 2C,2D*) were as follows: Ki-67 (35%), p16 (–),

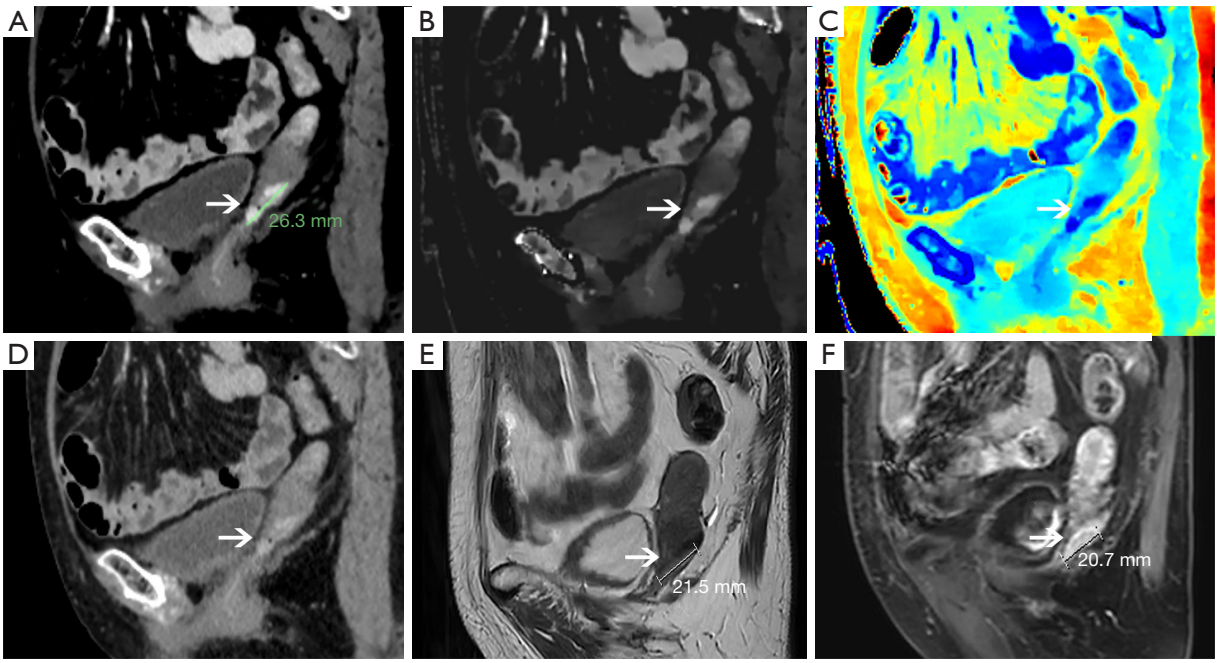

Figure 1 The images of dual-layer spectral detector CT, conventional CT in the venous phase, and MRI of case 1. (A) A virtual monoenergetic image 40 keV. The lesion shows an obvious enhancement with a clear boundary and the longest length of about 26 mm. (B) Iodine density map; (C) Z-effective map; (D) venous phase of conventional image, the focus shows mild enhancement, and its boundary is not clearly displayed; (E) T2WI, and the lesion shows hyperintensity with a length of about 22 mm; (F) enhanced T1WI, and the focus shows obvious enhancement with a length of about 21 mm. The white arrows indicate the lesion. CT, computed tomography; MRI, magnetic resonance imaging; T2WI, T2-weighted image; T1WI, T1-weighted image.

Table 1 Quantitative parameters of each image in each period of dual-layer spectral detector CT scan for the major lesion

Case #	Image sequence	Nonenhanced CT	Arterial phase	Venous phase
Case 1	Conventional image (HU)	46	96	108.5
	MonoE 40 keV (HU)	63	253	264.8
	Z-effective	7.42	8.64	8.65
	Iodine density (mg/mL)	0.26	2.59	2.62
	Iodine no water (mg/mL)	0.25	1.48	2.01
Case 2	Conventional image (HU)	45	84	59.8
	MonoE 40 keV (HU)	66	248	240
	Z-effective	7.47	8.59	8.50
	Iodine density (mg/mL)	0.33	2.47	2.30
	Iodine no water (mg/mL)	0.24	1.12	2.33

CT, computed tomography; HU, Hounsfield unit; MonoE, monoengetic image.

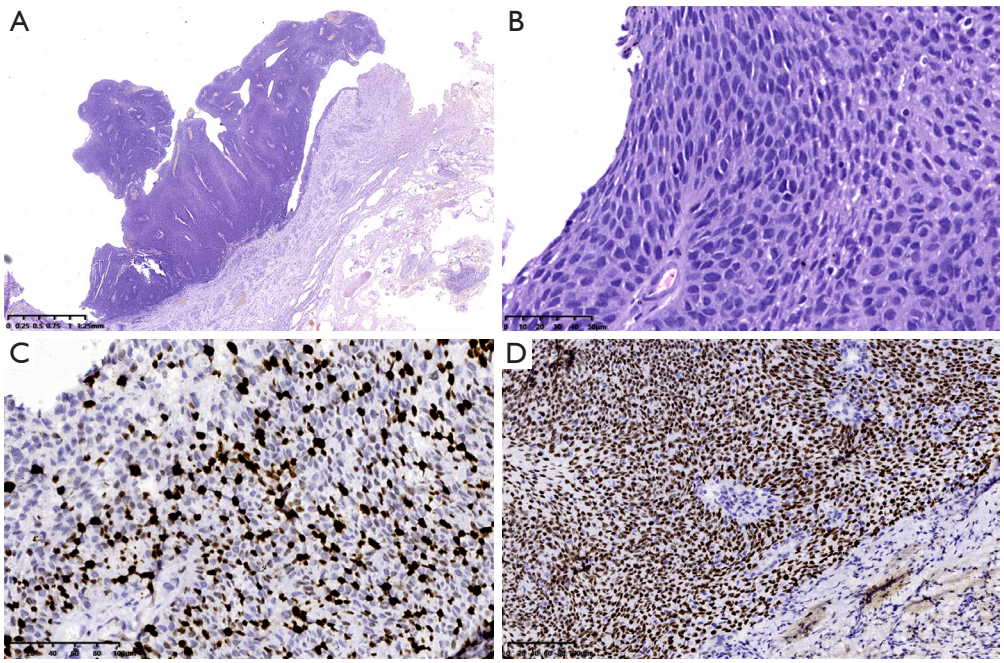

Figure 2 The images of pathological and immunohistochemical results of case 1. The standard protocols of histological analysis and EnVision Plus immunohistochemical staining were conducted. (A) Pathology showed that the squamous epithelium had an exophytic papillary hyperplasia. (B) H&E staining of the lesion. The lesion shows full thickness basal/parabasal-type atypia without an appreciable different and Atypic mitosis. (C) Positive staining for Ki-67 (MaxVision staining). (D) Nuclear positive staining for p40 (MaxVision staining). H&E, hematoxylin and eosin.

p53 (wild type), p63 (+), CK5/6 (focal +), S100 (individual positive), HMB45 (–), MART-1 (–), P40 (+), Sox-10 (–). After the surgery, the patient's vital signs were stable, and she had no vaginal bleeding. During 8 months after the surgery, the patient did not report any abnormal symptoms.

Case 2

A 72-year-old female had been diagnosed with vaginal melanoma 1 year ago. The tumor was resected and regular immunotherapies (acitinib and trepril) were undertaken. No abnormality was found during the follow-up pelvic CT plain and enhanced scans. Recently, the patient reported having experienced occasional vaginal bleeding 2 months. Gynecological physical examination showed masses in the front wall of the vagina, the middle of the right wall, and superior 1/3 of the right wall.

A pelvic DLCT examination was performed. Obvious and persistent enhancement in the upper, middle, and lower segments of the vagina were found on MonoE 40 keV, Z-effective map and ID map in the arterial phase (*Figure 3A-3C*), which had been missed by radiologists in conventional images (*Figure 3D*). In the venous phase, the abnormal enhancement range was extended, and the upper and lower part of the lesion showed a clearer boundary on MonoE 40 keV and ID map. The corresponding quantitative parameters are shown in *Table 1*. Pelvic MRI performed 6 days later (*Figure 3E,3F*) showed a lesion consistent with that observed on MonoE 40 keV. The maximum length of the lesion in MRI was 36 mm, the same with that on MonoE 40 keV. Positron emission tomography (PET) also showed the lesions in the vaginal wall and cervix.

The patient underwent surgery 3 days later. Irregular masses on the anterior and posterior wall of the vagina were pathologically diagnosed as malignant melanoma (posterior and anterior vaginal wall) with sheets or expansive nodules, and the tumor cells were spindled or epithelioid. The atypical mitosis was obvious (*Figure 4A,4B*). The largest lesion measured about 3.7 cm × 2.5 cm × 1.9 cm. The immunohistochemical results (*Figure 4C,4D*) were as follows: HMB45 (+), MART-1 (+), S100 (+), vimentin (+), Ki-67 (60%), p53 (mutant), CK (Pan) (–), Sox-10 (+). After

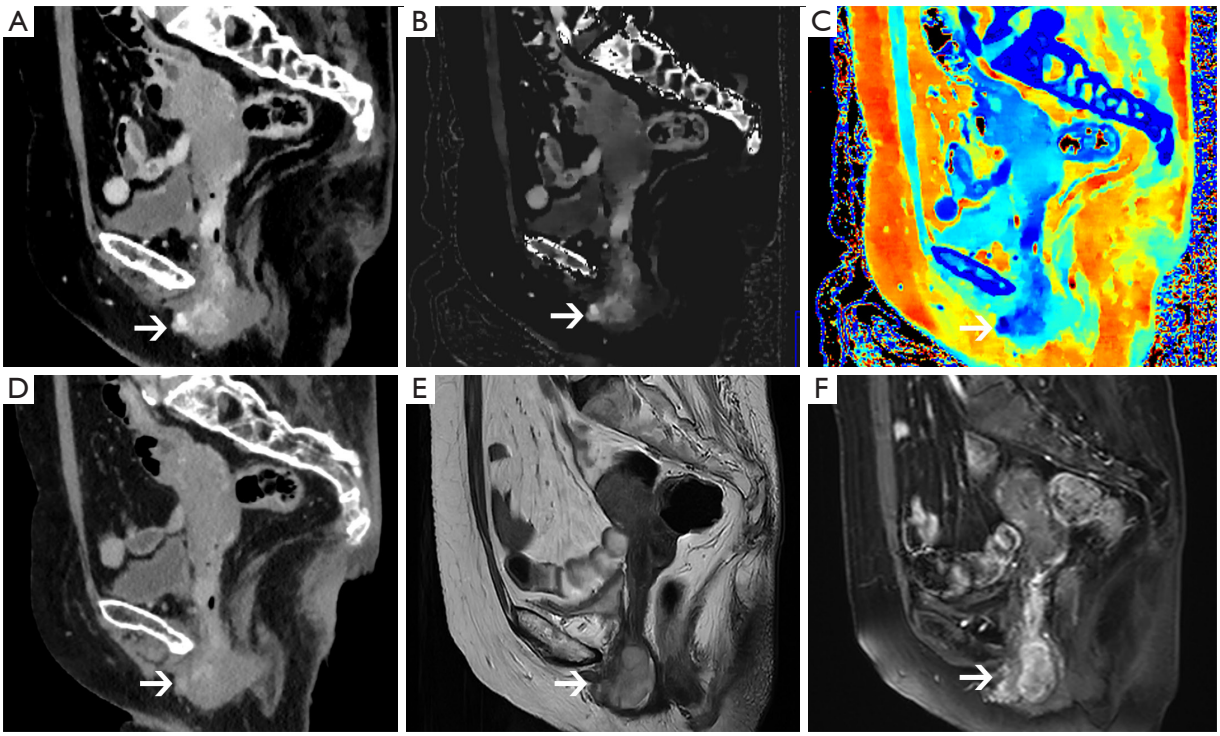

Figure 3 The images of dual-layer spectral detector CT, conventional CT in the venous phase, and MRI of case 2. (A) A virtual monoenergetic image at 40 keV. The lesion shows an obvious enhancement with unclear boundary, involving the lower, middle and upper segments of the vagina and a little posterior wall of cervix. (B) Iodine density map, which can clearly show the mass; (C) Z-effective map, which can clearly show the lesion area and the range of lesion involvement; (D) the venous phase of conventional image, the lesion is mild to moderate enhancement, and its boundary is not clearly displayed especially the lower part; (E) T2WI, the lesion shows hyperintensity and with a clear boundary, and the involved area of cervix is not clearly displayed; (F) enhanced T1WI, and the lesion shows obvious enhancement with abnormal linear enhancement of the posterior wall of the cervix. The white arrows indicate the lesion. CT, computed tomography; MRI, magnetic resonance imaging; T2WI, T2-weighted image; T1WI, T1-weighted image.

the surgery, the patient's vital signs were stable and she was discharged in 11 days. She received immunotherapy at a local hospital.

The images and signal-to-noise ratios (SNRs) of the lesions on the conventional and virtual monoenergetic images are demonstrated in the *Figure 5* and *Table 2*. It was revealed that the lesions showed the highest density on MonoE 40 keV and its SNR was also the highest.

All procedures performed in this study were in accordance with the ethical standards of the institutional and/or national research committee(s) and with the Helsinki Declaration (as revised in 2013). Written informed consent was provided by the patients for publication of this case report and accompanying images. A copy of the written consent is available for review from the editorial office of this journal.

Discussion

According to literature review, this is the first report for the detection of vaginal neoplasm using DLCT. In these two cases, compared with conventional images, the MonoE 40 keV, ID, and Z-effective map in DLCT increased the lesion detection and showed the boundary more clearly, especially on the venous phase. MonoE 40 keV offered a similar lesion size to that of MRI. DLCT holds the potential to improve lesion characterization and therapy monitoring, especially in oncologic management. It contributed on the differentiation of malignance even though in the small lesions via MonoE, ID mapping, and iodine overlay images (8). It also has the capability of improving subjective and objective image quality for the detection of metastases by using MonoEs of 40–70 keV (6). DLCT could provide various spectral parameters via different calculated maps. Quantitative ID on

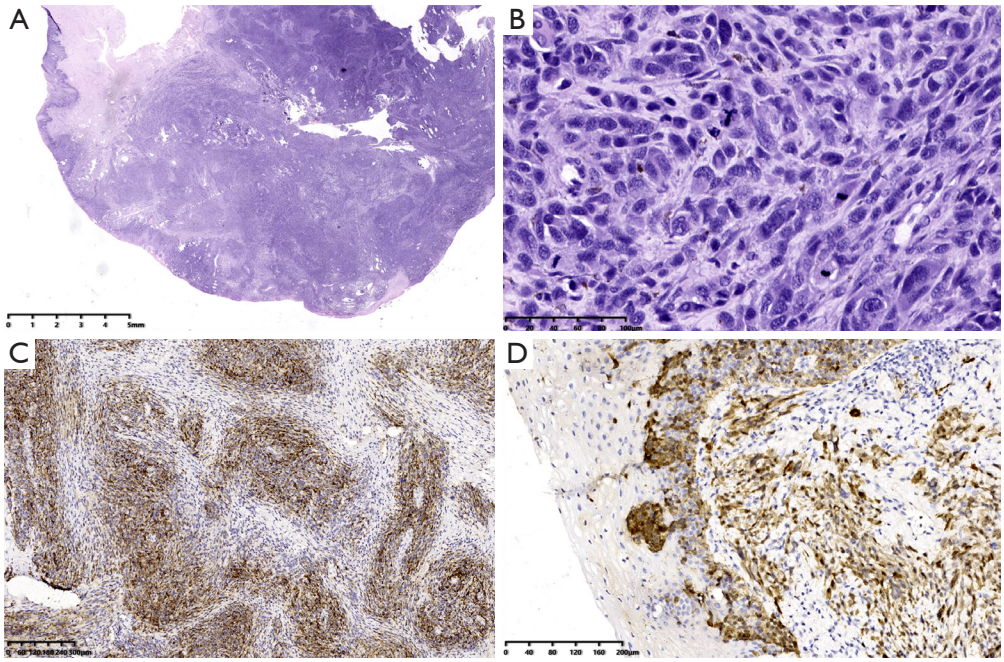

Figure 4 The images of pathological and immunohistochemical results of case 2. The standard protocols of histological analysis and EnVision Plus immunohistochemical staining were conducted. (A) Pathology showed sheets or expansive nodules. (B) H&E staining of the lesion. The tumor cell shows spindle or epithelioid, and atypical mitosis. (C) The tumor nucleus and cytoplasm positive staining for S100 (MaxVision staining). (D) Cytoplasm positive staining for HMB45 (MaxVision staining). H&E, hematoxylin and eosin.

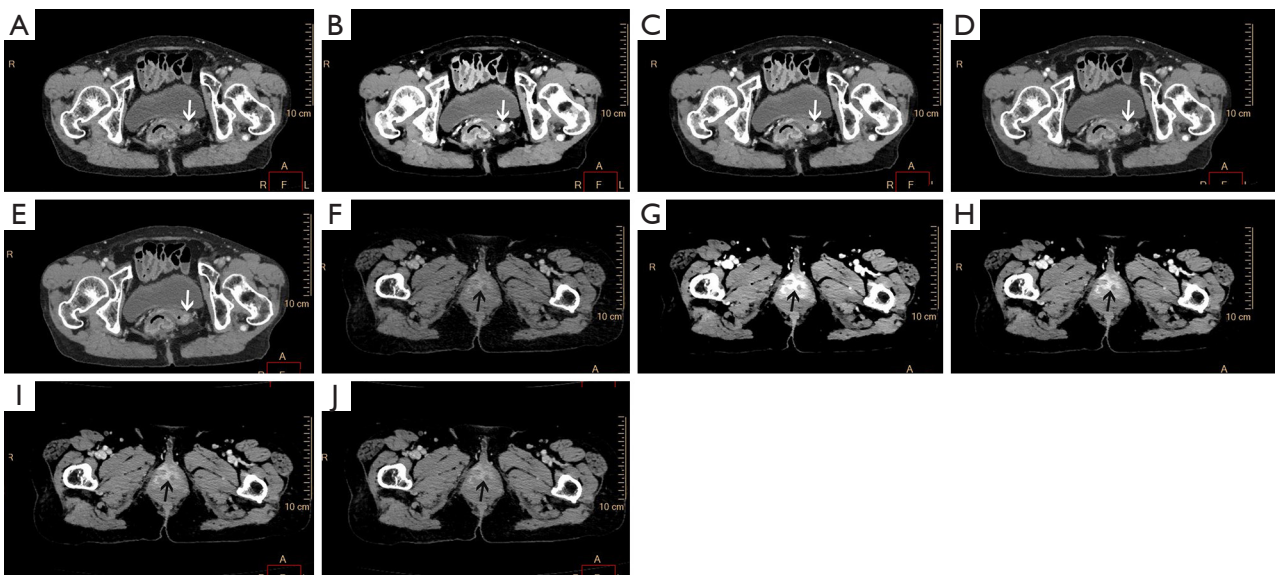

Figure 5 The comparation of conventional images and virtual monoenergetic images. (A-E) The conventional images and virtual monoenergetic images at 40, 50, 60, and 70 keV of the first patient, respectively. The white arrows indicate the enhancement of the lesions. (F-J) The conventional images and virtual monoenergetic images at 40, 50, 60, and 70 keV of the second patient, respectively. The black arrows indicate the large abnormal enhancement in the vagina.

Table 2 The SNRs of the lesions on the conventional and virtual monoenergetic images

Case #	Conventional image	MonoE 40 keV	MonoE 50 keV	MonoE 60 keV	MonoE 70 keV
Case 1	7.38	10.24	9.30	8.40	7.45
Case 2	7.02	15.90	12.44	9.99	8.22

SNRS, signal-to-noise ratios; MonoE, monoenergetic image.

non-enhanced CT image can predict tumor responses after a conventional transarterial chemoembolization procedure (9). Additionally, there are other potential advantages of DLCT. Firstly, compared with MRI, CT can carry out thinner slices and a variety of post-processing, which allows a more precise display of the longest diameter of a lesion. Secondly, since virtual non-contrast (VNC) images can be reconstructed on DLCT with enhanced scan, one venous phase scan may be sufficient, which could dramatically reduce the radiation dose (10,11). Thirdly, DLCT has potential value in the melanoma metastasis screening, as previously reported (12).

In conclusion, DLCT holds potential in the clinical management of vaginal neoplasm. It may be an efficient method for early diagnosis and follow-up of PVMs. In this study, MonoE 40 keV, ID, and Z-effective map on the venous phase were helpful in detecting PVMs and revealing its boundary. There are also some limitations in this case report. Firstly, the pictures of their gross specimens were lost, so that the description was only based on the literal documents. Secondly, the lymph nodes with suspected metastatic signs on PET images in case 2 were not resected in surgery; the value of DLCT in differentiating the malignance of lymph nodes was not assessed.

The primary "take-away" lessons are as follows:

(I) MonoE 40 keV, ID, and Z-effective map on the venous phase show their potential values in detecting PVMs and revealing its boundary.

(II) DLCT scan may be an efficient method for early diagnosis and follow-up of PVMs.

Acknowledgments

We want to acknowledge the contribution of Chen Ke who helped to perform the post-construction of the pictures.

Funding: This work was supported by the National Key R&D Program of China (No. 2022YFC2010000), the Key Program of National Natural Science Foundation of China (No. 81930049), the National Natural Science Foundation of China (No. 82271994), and Shanghai Science and Technology Innovation Action Plan Program (No. 19411951300).

Footnote

Conflicts of Interest: All authors have completed the ICMJE uniform disclosure form (available at https://qims.amegroups.com/article/view/10.21037/qims-23-717/coif). X.Z. reports that she is an employee of Philips Healthcare Greater. S.L. reports that this work was supported by the National Key R&D Program of China (No. 2022YFC2010000), the Key Program of National Natural Science Foundation of China (No. 81930049), and Shanghai Science and Technology Innovation Action Plan Program (No. 19411951300). Y.X. reports that this work was supported by the National Natural Science Foundation of China (No. 82271994). The other authors have no conflicts of interest to declare.

Ethical Statement: The authors are accountable for all aspects of the work in ensuring that questions related to the accuracy or integrity of any part of the work are appropriately investigated and resolved. All procedures performed in this study were in accordance with the ethical standards of the institutional and/or national research committee(s) and with the Helsinki Declaration (as revised in 2013). Written informed consent was provided by the patients for publication of this case report and accompanying images. A copy of the written consent is available for review by the editorial office of this journal.

References

1. Dunne EF, Park IU. HPV and HPV-associated diseases. Infect Dis Clin North Am 2013;27:765-78.
2. WHO Classification of Tumours·5th Edition--Female Genital Tumours. Available online: https://www.iarc.who.int/research-groups-esc-wct-keypublications/
3. McCluggage WG, Singh N, Gilks CB. Key changes to the World Health Organization (WHO) classification of female genital tumours introduced in the 5th edition (2020). Histopathology 2022;80:762-78.
4. Hu DN, Yu GP, McCormick SA. Population-based incidence of vulvar and vaginal melanoma in various races and ethnic groups with comparisons to other site-specific melanomas. Melanoma Res 2010;20:153-8.
5. El Kayal N, Lennartz S, Ekdawi S, Holz J, Slebocki K, Haneder S, Wybranski C, Mohallel A, Eid M, Grüll H, Persigehl T, Borggrefe J, Maintz D, Heneweer C. Value of spectral detector computed tomography for assessment of pancreatic lesions. Eur J Radiol 2019;118:215-22.
6. Nagayama Y, Iyama A, Oda S, Taguchi N, Nakaura T, Utsunomiya D, Kikuchi Y, Yamashita Y. Dual-layer dual-energy computed tomography for the assessment of hypovascular hepatic metastases: impact of closing k-edge on image quality and lesion detectability. Eur Radiol 2019;29:2837-47.
7. Obmann MM, An C, Schaefer A, Sun Y, Wang ZJ, Yee J, Yeh BM. Improved Sensitivity and Reader Confidence in CT Colonography Using Dual-Layer Spectral CT: A Phantom Study. Radiology 2020;297:99-107.
8. Laukamp KR, Tirumani SH, Lennartz S, Hokamp NG, Gupta A, Pennig L, Persigehl T, Gilkeson R, Ramaiya N. Evaluation of equivocal small cystic pancreatic lesions with spectral-detector computed tomography. Acta Radiol 2021;62:172-81.
9. Choi WS, Chang W, Lee M, Hur S, Kim HC, Jae HJ, Chung JW, Choi JW. Spectral CT-Based Iodized Oil Quantification to Predict Tumor Response Following Chemoembolization of Hepatocellular Carcinoma. J Vasc Interv Radiol 2021;32:16-22.
10. Connolly MJ, McInnes MDF, El-Khodary M, McGrath TA, Schieda N. Diagnostic accuracy of virtual non-contrast enhanced dual-energy CT for diagnosis of adrenal adenoma: A systematic review and meta-analysis. Eur Radiol 2017;27:4324-35.
11. Nagayama Y, Inoue T, Oda S, Tanoue S, Nakaura T, Ikeda O, Yamashita Y. Adrenal Adenomas versus Metastases: Diagnostic Performance of Dual-Energy Spectral CT Virtual Noncontrast Imaging and Iodine Maps. Radiology 2020;296:324-32.
12. Uhrig M, Simons D, Bonekamp D, Schlemmer HP. Improved detection of melanoma metastases by iodine maps from dual energy CT. Eur J Radiol 2017;90:27-33.

Cite this article as: Cui Y, Zhang Z, Zhang X, Zhao B, Shi X, Zhu Z, Liu X, Liu S, Xiao Y. Imaging findings of primary vaginal malignancies by dual-layer spectral detector CT: description of two patients. Quant Imaging Med Surg 2024;14(1):1245-1251. doi: 10.21037/qims-23-717

